Asymptotic behavior of the isotropic-nematic and nematic-columnar phase boundaries for the system of hard rectangles on a square lattice

Joyjit Kundu* and R. Rajesh†
The Institute of Mathematical Sciences, C.I.T. Campus, Taramani, Chennai 600113, India
(Received 16 September 2014; published 6 January 2015)

A system of hard rectangles of size $m \times mk$ on a square lattice undergoes three entropy-driven phase transitions with increasing density for large-enough aspect ratio k: first from a low-density isotropic to an intermediate-density nematic phase, second from the nematic to a columnar phase, and third from the columnar to a high-density sublattice phase. In this paper we show, from extensive Monte Carlo simulations of systems with $m = 1,2$, and 3, that the transition density for the isotropic-nematic transition is $\approx A_1/k$ when $k \gg 1$, where A_1 is independent of m. We estimate $A_1 = 4.80 \pm 0.05$. Within a Bethe approximation and virial expansion truncated at the second virial coefficient, we obtain $A_1 = 2$. The critical density for the nematic-columnar transition when $m = 2$ is numerically shown to tend to a value less than the full packing density as k^{-1} when $k \to \infty$. We find that the critical Binder cumulant for this transition is nonuniversal and decreases as k^{-1} for $k \gg 1$. However, the transition is shown to be in the Ising universality class.

DOI: 10.1103/PhysRevE.91.012105 PACS number(s): 64.60.De, 64.60.Cn, 05.50.+q

I. INTRODUCTION

Hard-core lattice gas models of particles interacting only through excluded volume interaction continue to be of interest in statistical physics. They are minimal models to study entropy-driven phase transitions, have direct realizations in adsorption of gas particles on metal surfaces [1–6], and are closely related to the freezing transition [7,8], directed and undirected animals [9–11], and the Yang-Lee singularity [12]. Systems of differently shaped particles on different lattices have been studied both analytically and numerically. Examples include squares [13–18], hexagons [19,20], dimers with nearest neighbor exclusion [21], triangles [22], tetrominoes [23], rods [24,25], rectangles [26], lattice models for disks [27,28], and mixtures [29].

In this paper, we focus on the system of hard rectangles of size $m \times mk$ on the square lattice, where each rectangle occupies m sites along the short axis and mk sites along the long axis, where k is the aspect ratio and m, k are integers. In recent times, there has been renewed interest in this problem when, even though both the low-density and the maximal-density phases are known to be disordered [30], the existence of a nematic phase for the hard-rod ($m = 1$) system was convincingly demonstrated in simulations for $k \geqslant 7$ [24] and thereafter proven rigorously for $k \gg 1$ [31]. The maximal-density phase being disordered implies the existence of a second entropy-driven transition with increasing density. This has been established in simulations using an algorithm that involves cluster moves [25]. The first transition from the isotropic phase to the nematic phase has been shown to be in the Ising universality class numerically in two dimensions [32,33] and through an exact solution in large dimensions. [34]. However, the universality class of the second transition from the nematic phase to the high-density disordered phase is not that clear [25,35]. Though the numerically obtained exponents differ from those of the Ising model, it is not possible to rule out a crossover to Ising exponents at larger length scales [25].

The phase diagram for rectangles with $m > 1$ is even richer and was recently determined using Monte Carlo simulations for $m = 2,3$ and $k \leqslant 7$ and generalized to larger m,k using arguments based on estimates of entropy for the different phases [26]. When the aspect ratio $k = 1$ and $m \geqslant 2$, the model reduces to the well-studied hard-square model which undergoes a single density-driven transition from from a low-density isotropic phase to a high-density columnar phase [14,18]. The transition is continuous for $m = 2$ [17,27,36] and first order for $m = 3$ [27]. For $k \geqslant 7$ and $m \geqslant 2$, with increasing density, the system transits successively from isotropic (I) to nematic (N) to columnar (C) to solidlike sublattice (S) phases (see Sec. II for a precise define of the phases). When $k < 7$, the N phase is absent. For $2 \leqslant k < 7$ when $m \geqslant 3$, and for $4 \leqslant k < 7$ when $m = 2$, the system undergoes two transitions with increasing density: first from the I phase to the C phase and, second, from the C phase to the S phase. The C phase does not exist for $k = 2,3$ when $m = 2$, and the system makes a direct transition from the I phase to the S phase. A detailed study of the nature of the transitions may be found in Ref. [26].

In this paper, we focus on the asymptotic behavior of the isotropic-nematic (I-N) and nematic-columnar (N-C) phase boundaries for large aspect ratio k. It was heuristically argued in Ref. [26] that the limit $k \to \infty$, keeping m fixed, should correspond to the limit of oriented lines in the continuum, and thus the critical density should be independent of m. For this limiting case in three dimensions, the virial expansion truncated at the second virial coefficient becomes exact and the critical density for the I-N transition $\rho_c^{I-N} \approx A_1 k^{-1}$ [37–39]. A_1 for oriented long rectangles in the two-dimensional continuum can be directly estimated by simulating oriented lines of length ℓ, for which it is straightforward to show that the critical number density $\approx A_1 \ell^{-2}$. From the simulations of this system with $\ell = 1$, it can be inferred that $A_1 \approx 4.84$ [33]. For $m = 1$, by simulating systems with k up to 12 on the lattice, it has been shown that $\rho_c^{I-N} \propto k^{-1}$ [40].

*joyjit@imsc.res.in
†rrajesh@imsc.res.in

From the value of the critical density for $k = 10$ [40], it can be estimated that $A_1 \approx 5.02$, which differs from that for oriented lines [33]. There are no such similar studies for $m > 1$.

For the N-C transition, the limit $k \to \infty$, keeping m fixed, corresponds to asking whether oriented long rectangles in the continuum exhibit a C phase. The N-C transition has been studied using a Bethe approximation that predicts the critical density to be $\rho_c^{N-C} \approx A_2(m) + A_3(m)k^{-1}$ when $k \to \infty$, where $A_2(m) \leqslant 1$ [26]. These results are consistent with those obtained from truncated high-activity expansions [41]. The approximations being *ad hoc*, it is important to have numerical confirmation of these results, but none exists. The other limit $m \to \infty$, keeping k fixed, corresponds to the continuum problem of oriented rectangles of aspect ratio k, a model that was introduced and studied by Zwanzig using virial expansion [38]. This limit is difficult to study numerically on the square lattice.

In this paper, by simulating systems of rectangles with aspect ratio k up to 60 (for $m = 1$), and $k = 56$ (for $m = 2$ and 3), we show that ρ_c^{I-N} is proportional to k^{-1} for $m = 1,2$, and 3. Within numerical error, A_1 is shown to be independent of m and equal to 4.80 ± 0.05. To understand better the limit of large k, we study the I-N transition using a Bethe approximation, and a virial expansion truncated at the second virial coefficient. The critical density ρ_c^{I-N} is obtained for all m and k. When k is large, both the theories predict that $\rho_c^{I-N} \approx A_1/k$, where $A_1 = 2$. In particular, we find that within the virial expansion truncated at the second virial coefficient, ρ_c^{I-N} is independent of m, for all k. For the N-C transition, we numerically determine ρ_c^{N-C} for $m = 2$ and k up to 24. We show that for large k, $\rho_c^{N-C} \approx 0.73 + 0.23k^{-1}$, consistent with the calculations in Ref. [26]. This shows that a system of oriented rectangles with large aspect ratio in the two-dimensional continuum should exhibit both nematic and columnar phases. In addition, we find that the Binder cumulant at the N-C transition is surprisingly dependent on k and decreases as k^{-1} with increasing k. However, we show that the transition remains in the Ising universality class.

The rest of the paper is organized as follows. Section II contains a definition of the model, a brief description of the Monte Carlo algorithm, and a definition of the phases and the relevant thermodynamic quantities of interest. In Sec. III, we present the numerical results for the I-N transition for $m = 1,2$, and 3. In Sec. IV, we numerically determine the asymptotic behavior of the N-C phase boundary for $m = 2$ and large k. The Binder cumulant is shown to be nonuniversal, though exponents continue to be universal. Section V contains calculations of the I-N phase boundary using an *ad hoc* Bethe approximation and a truncated virial expansion. Section VI contains a summary and discussion of results.

II. MODEL AND DEFINITIONS

We consider a system of monodispersed hard rectangles of size $m \times mk$ on a square lattice of size $L \times L$, with periodic boundary conditions. Each rectangle occupies m sites along the short axis and mk sites along the long axis, such that k is the aspect ratio. A rectangle is called horizontal or vertical depending on whether the long axis is along the x axis or y axis. No two rectangles may overlap, or, equivalently, a lattice site may be occupied by utmost one rectangle. We associate an activity $z = e^{\mu}$ to each rectangle, where μ is the chemical potential.

We simulate the system in the constant μ grand-canonical ensemble using an efficient algorithm that involves cluster moves. The implementation of the algorithm for the system of hard rectangles is described in detail in Ref. [26]. Here we briefly review the algorithm. Starting with an arbitrary configuration of rectangles, a row (or a column) is chosen at random. First, all the horizontal (vertical) rectangles whose bottom left corners are on that row (column) are evaporated, keeping the remaining rectangles as they are. The row (column) now consists of intervals of empty sites, separated by sites which are either already occupied by rectangles or cannot be occupied due to the hard-core constraint. Next, the empty intervals of the row (column) are refilled by deposition of horizontal (vertical) rectangles with the correct equilibrium grand canonical probabilities. The calculation of these probabilities reduces to a solvable one-dimensional problem. In addition to the evaporation-deposition move, we also implement a flip move. In this move, a site is picked up at random. If the chosen site is occupied by the head of a horizontal (vertical) rectangle, we look for a square plaquette of size $mk \times mk$ consisting of k aligned horizontal (vertical) rectangles. If such a plaquette exists, it is replaced by a similar plaquette of k vertical (horizontal) rectangles. One Monte Carlo move corresponds to $2L$ evaporation-deposition and L^2 plaquette flip moves. The algorithm has been shown to be very useful in equilibrating hard-core systems of extended particles at high densities. Other implementations of the algorithm include lattice models of hard rods [25,42] and hard disks [28] and mixtures of dimers and hard squares [29].

The data presented in the paper corresponds to systems with aspect ratio up to 60 and system sizes up to $L = 1680$. In the simulations, we ensured equilibration by confirming that the final state is independent of the initial configuration. The system is typically equilibrated for 10^7 Monte Carlo steps, and the measurement is broken into 10 statistically independent blocks, each of size 10^7 Monte Carlo steps.

The system of hard rectangles may exist in one of the four different phases: isotropic (I), nematic (N), columnar (C), and sublattice (S) [26]. In the low-density I phase the system neither possess orientational order nor positional order. The N phase breaks the orientational symmetry by preferring a particular orientation, either horizontal or vertical. However, the N phase has no positional order. In the C phase, along with orientational order, the system possesses partial positional order in the direction perpendicular to the preferred orientation. In the C phase of $2 \times 2k$ rectangles, if most of the rectangles are horizontal (vertical), then the heads (bottom left corner) of the rectangles mostly occupy either even or odd rows (columns). The high-density S phase has positional order along both horizontal and vertical directions, but no orientational order. In this phase the heads of the rectangles preferentially occupy one of m^2 sublattices [26].

We now define the order parameters and relevant thermodynamic quantities used to study the I-N and the N-C transitions.

For the I-N transition, we define a order parameter

$$Q_1 = \frac{\langle |N_h - N_v| \rangle}{\langle N_h + N_v \rangle}, \tag{1}$$

where N_h and N_v are the number of horizontal and vertical rectangles respectively. Q_1 is zero in the I phase and nonzero in the N and C phases. For the N-C transition, we define an order parameter only for $m = 2$ as our simulations are restricted to this value of m. Generalization to larger m is straightforward [26]. Let

$$Q_2 = \frac{\langle ||N_{\rm re} - N_{\rm ro}| - |N_{\rm ce} - N_{\rm co}|| \rangle}{\langle N_h + N_v \rangle}, \tag{2}$$

where $N_{\rm re}$ ($N_{\rm ro}$) is the number of rectangles whose heads are in the even (odd) rows, and $N_{\rm ce}$ ($N_{\rm co}$) is the number of rectangles whose heads are in the even (odd) columns. In the I and N phases, $N_{\rm re} \approx N_{\rm ro}$, and $N_{\rm ce} \approx N_{\rm co}$, and hence Q_2 is zero. In the C phase, either $N_{\rm re} \neq N_{\rm ro}$ and $N_{\rm ce} \approx N_{\rm co}$, or $N_{\rm re} \approx N_{\rm ro}$ and $N_{\rm ce} \neq N_{\rm co}$, such that Q_2 is nonzero.

The second moment of the order parameter χ_i and the Binder cumulant U_i are defined as

$$\chi_i = \langle Q_i^2 \rangle L^2, \tag{3a}$$

$$U_i = 1 - \frac{\langle Q_i^4 \rangle}{3\langle Q_i^2 \rangle^2}, \tag{3b}$$

where $i = 1,2$. The thermodynamic quantities become singular at the transition. Let $\epsilon = (\mu - \mu_c)/\mu_c$, where μ_c is the critical chemical potential. The singular behavior is characterized by the critical exponents β, γ, ν defined by $Q_i \sim (-\epsilon)^\beta$, $\epsilon < 0$, $\chi_i \sim |\epsilon|^{-\gamma}$, and $\xi_i \sim |\epsilon|^{-\nu}$, where ξ_i is the correlation length, $|\epsilon| \to 0$, and $i = 1,2$. The critical exponents may be obtained numerically through finite-size scaling near the critical point:

$$U_i \simeq f_u(\epsilon L^{1/\nu}), \tag{4a}$$

$$Q_i \simeq L^{-\beta/\nu} f_q(\epsilon L^{1/\nu}), \tag{4b}$$

$$\chi_i \simeq L^{\gamma/\nu} f_\chi(\epsilon L^{1/\nu}), \tag{4c}$$

where f_u, f_q, and f_χ are scaling functions.

III. ASYMPTOTIC BEHAVIOR OF THE ISOTROPIC-NEMATIC PHASE BOUNDARY: NUMERICAL STUDY

In this section we investigate the asymptotic behavior of the I-N phase boundary for $m = 1$, 2, and 3 by numerical simulations and show that $\rho_c^{I-N} = A_1 k^{-1}$ when $k \gg 1$, where A_1 is independent of m. Since there are two symmetric N phases (horizontal and vertical), the I-N transition for the system of hard rectangles is continuous and belongs to the Ising universality class for all m [26]. We determine the critical density ρ_c^{I-N} from the point of intersection of the curves of Binder cumulant with density for different system sizes. A typical example is shown in Fig. 1, where the variation of U_1 with density ρ is shown for three different system sizes when $m = 1$ and $k = 32$. The Binder cumulant data are fitted to a cubic spline to obtain a smooth and continuous curve for each L. This allows us to determine the point of intersection

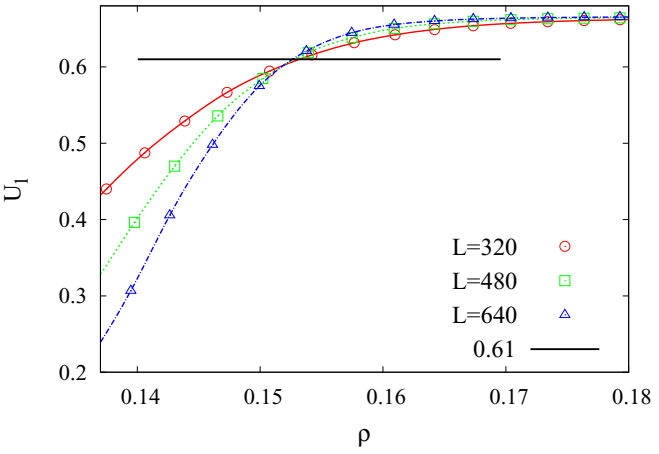

FIG. 1. (Color online) The variation of the Binder cumulant U_1 with density ρ for three different system sizes. The lines are cubic splines, fitted to the data. The value of U at $\rho = \rho_c$ is ≈ 0.61. The data are for $m = 1$ and $k = 32$.

or ρ_c^{I-N} more accurately. In the example shown in Fig. 1, the curves for Binder cumulants for three different system sizes crosses at $\rho = \rho_c^{I-N} \approx 0.152$ and the value of the critical Binder cumulant $U_1^c \approx 0.61$. We find $U_1^c \approx 0.61$ for all values of m and k that we have studied, consistent with the value for the two-dimensional Ising model [43].

We simulate systems with aspect ratio up to $k = 60$ for $m = 1$ and $k = 56$ for $m = 2$ and 3. The critical density ρ_c^{I-N} obtained from the Binder cumulants are shown in Fig. 2. The data are clearly linear in k^{-1} for large k, confirming that $\rho_c^{I-N} = A_1 k^{-1}$, $k \gg 1$. In addition, the data for $m = 1,2,3$ asymptotically lie on the same straight line, showing that A_1 is independent of m. We estimate $A_1 = 4.80 \pm 0.05$.

IV. ASYMPTOTIC BEHAVIOR OF THE NEMATIC-COLUMNAR PHASE BOUNDARY: NUMERICAL STUDY

In this section, we numerically study the N-C phase transition for $m = 2$ and determine the asymptotic behavior

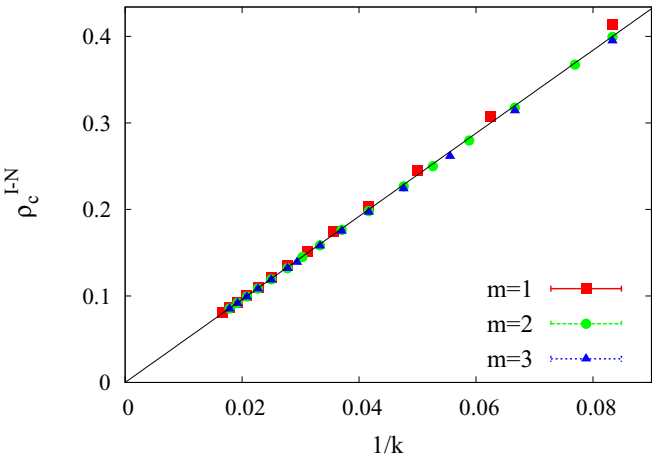

FIG. 2. (Color online) The variation of the critical density for the I-N transition ρ_c^{I-N} with k^{-1} for $m = 1,2$, and 3. The straight line is $4.80k^{-1}$.

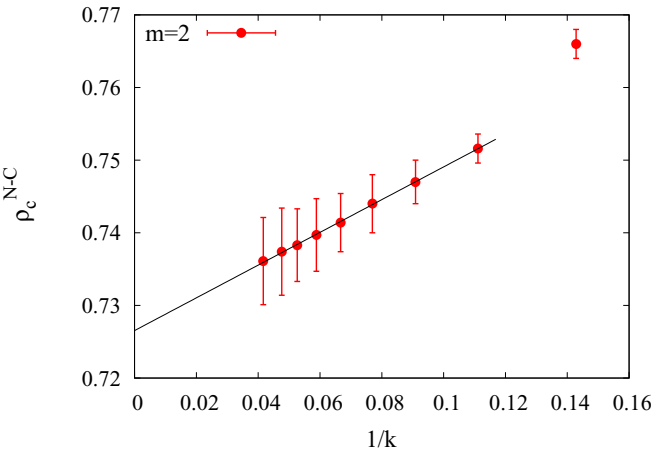

FIG. 3. (Color online) The variation of the critical density for the N-C transition ρ_c^{N-C} with k^{-1} for $m = 2$. The straight line is a linear fit to the data: $0.727 + 0.226k^{-1}$.

of the critical density ρ_c^{N-C} for large k. When $m = 2$, the N-C transition belongs to the Ising universality class for all k and the corresponding critical densities are determined from the intersection of Binder cumulant curves for different system sizes as discussed in Sec. III.

The critical density ρ_c^{N-C} decreases to a constant with increasing k (see Fig. 3). We obtain $\rho_c^{N-C} \approx 0.727 + 0.226k^{-1}$, $k \gg 1$ when $m = 2$. These results are in qualitative agreement with the predictions of the Bethe approximation: $\rho_c^{N-C} \approx A_2(m) + B_2(m)k^{-1}$, for $k \gg 1$. Within the Bethe approximation $A_2 \approx 0.59$ and $B_2 \approx 0.15$ for $m = 2$ [26]. As ρ_c^{N-C} asymptotically approaches a constant value, it becomes increasingly difficult to get reliable data for large k.

Surprisingly, we find that the value of the critical Binder cumulant at the N-C transition point depends on the aspect ratio k. When $m = 2$, the critical Binder cumulant U_2^c decreases monotonically as a power law with k, from 0.50 when $k = 7$ to 0.18 when $k = 24$ (see Fig. 4). The data is fitted best with $U_2^c \approx 4.45k^{-1}$. Usually, for the Ising universality class, the value

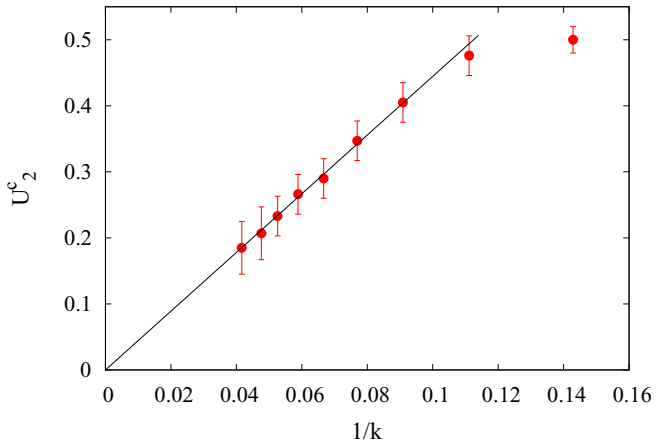

FIG. 4. (Color online) The variation of the critical Binder cumulant U_2^c at the N-C transition with k^{-1}. The straight line $4.446k^{-1}$ is a linear fit to the data. The data are for $m = 2$.

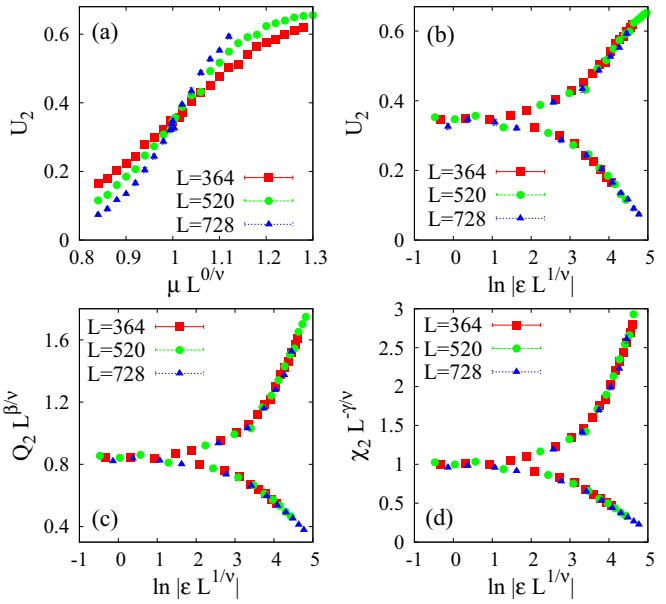

FIG. 5. (Color online) The critical behavior near the N-C transition for rectangles of size 2×26 ($k = 13$). (a) The data for Binder cumulant for different system sizes intersect at $\mu_c \approx 1.00$. The data for different L near the N-C transition for (b) Binder cumulant, (c) order parameter, and (d) second moment of the order parameter collapse onto a single curve when scaled as in Eq. (4) with the Ising exponents $\beta/\nu = 1/8$, $\gamma/\nu = 7/4$, and $\nu = 1$.

critical Binder cumulant at the transition point is expected to be universal (≈0.61). However, there are a few examples of systems that exhibit such nonuniversal behavior [43–45]. These include the anisotropic Ising model where the critical Binder cumulant depends on the ratio of the coupling constants along the x and y directions [44], and the isotropic Ising model on rectangular lattice, where the critical Binder cumulant is a function of the aspect ratio of the underlying lattice [43]. In the latter case, $U_2^c \approx 2.46\alpha^{-1}$, where α is the aspect ratio of the lattice [43]. Thus, nominally, $k \approx 1.8\alpha$.

Although U_2^c varies with k, we confirm that the critical exponents for the N-C transition remains the same as those of the two-dimensional Ising model. To do so, we determine the critical exponents for the system with $m = 2$ and $k = 13$ using finite-size scaling. For this example, critical Binder cumulant is ≈0.35, noticeably differs from that for the Ising universality class. The data for the Binder cumulant U_2 for different system sizes intersect at $\mu_c \approx 1.00$ [see Fig. 5(a)]. We find that the data for U_2, Q_2, and χ_2 for different system sizes collapse onto a single curve when scaled as in Eq. (4) with Ising exponents $\beta/\nu = 1/8$, $\gamma/\nu = 7/4$, and $\nu = 1$ [see Fig. 5(b)–5(d)]. We thus conclude that, though the critical Binder cumulant is nonuniversal, the transition is in the Ising universality class.

V. ESTIMATION OF THE I-N PHASE BOUNDARY USING ANALYTICAL METHODS

In this section we obtain the asymptotic behavior of the isotropic-nematic phase boundary for large k using analytical methods. In the absence of an exact solution, we present

two approximate calculations: first, a Bethe approximation and, second, a virial expansion truncated at the second virial coefficient.

A. Bethe approximation

The Bethe approximation becomes exact on treelike lattices. For $m = 1$, the model was solved exactly on the four-coordinated random locally treelike layered lattice (RLTL) to obtain $\rho_c^{I-N} = 2/(k-1)$ [34] or $A_1 = 2$. The RLTL also allows an exact solution to be obtained for more complicated systems like repulsive rods [35]. However, a convenient formulation of the problem of hard rectangles on the RLTL is lacking. Therefore, we resort to an *ad hoc* Bethe approximation introduced by DiMarzio to estimate the entropy of hard rods on a cubic lattice [46] and later used for studying the statistics of hard rods on different lattices [40,47,48]. However, a straightforward extension of this method to a system of rectangles suffers from the enumeration result depending on the order in which the rectangles are placed. A scheme that overcomes this shortcoming was suggested in Ref. [49] and was implemented by us to study the N-C transition [26]. Here, we adapt the calculations to study the I-N transition.

The I-N phase boundary can be determined if the entropy as a function of the densities of the horizontal and vertical rectangles is known. We estimate the entropy by computing the number of ways of placing N_x horizontal and N_y vertical rectangles on the lattice.

First, we place the horizontal rectangles on the lattice one by one. Given that j_x horizontal rectangles have been placed, the number of ways of placing the $(j_x+1)^{\text{th}}$ horizontal rectangle may be estimated as follows. The head of the rectangle may be placed in one of the $(M - m^2kj_x)$ empty sites, where M is the total number of lattice sites. We denote this site by A (see Fig. 6). For this new configuration to be valid, all sites in the $m \times mk$ rectangle with head at A should be empty. Given A is empty, we divide the remaining (m^2k-1) sites in three groups: $(mk-1)$ sites along the line AB, $(m-1)$ sites along the line AC, and the remaining $(m-1)(mk-1)$ sites (D is an example). Let $P_x(B|A)$ be the conditional probability that B is empty given that A is empty. Then the probability that $(mk-1)$ sites along the line AB are empty is $[P_x(B|A)]^{mk-1}$,

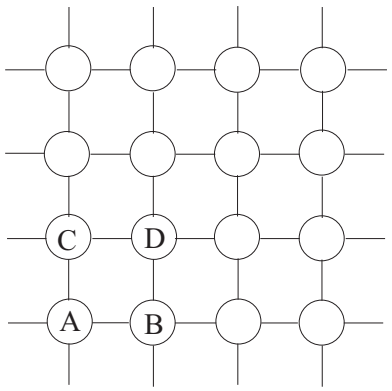

FIG. 6. Schematic of a square lattice showing the position of the sites A-B to explain the calculation of the isotropic-nematic phase boundary.

where the subscript x denotes the direction AB. In writing this, we ignore all correlations beyond the nearest neighbor. Likewise, the probability that $(m-1)$ sites along the line AC are empty is given by $[P_y(C|A)]^{m-1}$, where $P_y(C|A)$ is the conditional probability that C is empty given A is empty. Let $P(D|B \cap C)$ denote the conditional probability that D is empty given that B and C are both empty. Then the probability that the remaining $(m-1)(mk-1)$ sites are empty may be approximated by $[P(D|B \cap C)]^{(m-1)(mk-1)}$. Collecting these different terms together, we obtain the number of ways to place the $(j_x+1)^{\text{th}}$ horizontal rectangle

$$\nu_{j_x+1} = (M - m^2kj_x) \times [P_x(B|A)]^{mk-1}[P_y(C|A)]^{m-1} \times [P(D|B \cap C)]^{(m-1)(mk-1)}. \tag{5}$$

It is not possible to determine these conditional probabilities exactly. However, they may be estimated by assuming that the rectangles are placed randomly. Given A is empty, either B might be empty or occupied by a horizontal rectangle (as no vertical rectangles have been placed yet) in m ways. Thus, given A is empty, the probability that B is also empty, is

$$P_x(B|A) = \frac{M - m^2kj_x}{M - m^2kj_x + mj_x}. \tag{6}$$

Similarly, if A is empty, C might be empty or it might be occupied by any of the mk sites on the longer axis (passing through C) of a horizontal rectangle. Thus the probability that C is empty, given A empty is given by

$$P_y(C|A) = \frac{M - m^2kj_x}{M - m^2kj_x + mkj_x}. \tag{7}$$

Next we estimate $P(D|B \cap C)$. If we follow a similar approach to calculate $P(D|B \cap C)$, the resultant entropy becomes dependent on the order of placement of the horizontal and vertical rectangles and thus asymmetric with respect to N_x and N_y. To overcome this shortcoming, we follow the Bethe approximation proposed in Ref. [49] and assume

$$P(D|B \cap C) \approx \frac{P_x(C|D)P_y(B|D)}{P_{xy}(C|B)}, \tag{8}$$

where

$$P_{xy}(B|C) = \frac{M - m^2kj_x}{M - m(m-1)kj_x + (m-1)j_x}, \tag{9}$$

is the probability that C is empty given B is empty. It can be easily seen that

$$P_x(C|D) = P_x(B|A), \tag{10a}$$

$$P_y(B|D) = P_y(C|A). \tag{10b}$$

As all the horizontal rectangles are indistinguishable, the total number of ways to place N_x of them is

$$\Omega_x = \frac{1}{N_x!}\prod_{j_x=0}^{N_x-1}\nu_{j_x+1}. \tag{11}$$

Substituting Eqs. (6)–(10) into Eq. (5), we obtain ν_{j_x+1}. Ω_x is given by

$$\Omega_x = \frac{1}{N_x!}\prod_{j_x=0}^{N_x-1}\frac{[M-m^2kj_x]^{m^2k}[M-(m-1)(mk-1)j_x]^{(m-1)(mk-1)}}{[M-m(mk-1)j_x]^{m(mk-1)}[M-mk(m-1)j_x]^{mk(m-1)}}. \tag{12}$$

After placing N_x horizontal rectangles we would like to determine the number of ways in which N_y vertical rectangles may be placed on the lattice. Given N_x horizontal rectangles and j_y vertical rectangles have already been placed, we estimate ν_{j_y+1}, the number of ways to place the $(j_y+1)^{\text{th}}$ vertical rectangle, using the same procedure as above. Now, we may choose an empty site A (see Fig. 6) randomly in $(M-m^2kN_x-m^2kj_y)$ ways to place the head of the $(j_y+1)^{\text{th}}$ vertical rectangle. As the vertical rectangles have their longer axis along y direction, it can be easily seen that

$$\nu_{j_y+1} = (M-m^2kN_x-m^2kj_y)[P_y(C|A)]^{mk-1} \times [P_x(B|A)]^{m-1}[P(D|B\cap C)]^{(m-1)(mk-1)}. \tag{13}$$

The expressions for the conditional probabilities will now be modified due to the presence of both horizontal and vertical rectangles. If A is empty, C may be empty or occupied by one of the mk sites on the long axis (passing through C) of a horizontal rectangle or by one of the m sites on the short axis (passing through C) of a vertical rectangle. Hence, given A is empty, the probability that C is also empty is

$$P_y(C|A) = \frac{M-m^2kN_x-m^2kj_y}{M-mk(m-1)N_x-m(mk-1)j_y}. \tag{14}$$

Similarly, the probability of B being empty, given A is empty, is

$$P_x(B|A) = \frac{M-m^2kN_x-m^2kj_y}{M-m(mk-1)N_x-mk(m-1)j_y}. \tag{15}$$

Now the probability that B is empty, given C is empty, is

$$P_{xy}(B|C) = \frac{M-m^2kN_x-m^2kj_y}{M-(mk-1)(m-1)(N_x+j_y)}. \tag{16}$$

$P(D|B\cap C)$ is determined using Eqs. (8) and (10). Substituting Eqs. (14)–(16) into Eq. (13), we obtain ν_{j_y+1}. The total number of ways to place N_y vertical rectangles, given that N_x horizontal rectangles have already been placed, is then

$$\Omega_y = \frac{1}{N_y!}\prod_{j_y=0}^{N_y-1}\nu_{j_y+1} = \frac{1}{N_y!}\prod_{j_y=0}^{N_y-1}\frac{[M-m^2k(N_x+j_y)]^{m^2k}}{[M-m(mk-1)N_x+mk(m-1)j_y]^{mk(m-1)}} \times \frac{[M-(m-1)(mk-1)N_x-(m-1)(mk-1)j_y]^{(m-1)(mk-1)}}{[M-mk(m-1)N_x-m(mk-1)j_y]^{m(mk-1)}}. \tag{17}$$

The total number of ways to place N_x horizontal and N_y vertical rectangles on the lattice is given by

$$\Omega = \Omega_x\Omega_y. \tag{18}$$

Let ρ_x and ρ_y be the fraction of the sites occupied by the horizontal and the vertical rectangles, given by

$$\rho_i = \frac{m^2kN_i}{M}, \quad i = x,y. \tag{19}$$

Using Eqs. (12) and (17), the entropy of the system per site in the thermodynamic limit may be expressed in terms of ρ_x and ρ_y as

$$\begin{aligned} s(\rho_x,\rho_y) &= \lim_{M\to\infty}\frac{1}{M}\ln(\Omega_x\Omega_y) \\ &= -\sum_{i=x,y}\frac{\rho_i}{m^2k}\ln\frac{\rho_i}{m^2k} - [1-\rho]\ln[1-\rho] - \left[1-\frac{(m-1)(mk-1)}{m^2k}\rho\right]\ln\left[1-\frac{(m-1)(mk-1)}{m^2k}\rho\right] \\ &\quad + \sum_{i=x,y}\left[1-\frac{(mk-1)}{mk}\rho+\frac{(k-1)}{mk}\rho_i\right]\ln\left[1-\frac{(mk-1)}{mk}\rho+\frac{(k-1)}{mk}\rho_i\right], \end{aligned} \tag{20}$$

where $\rho = \rho_x+\rho_y$ is the fraction of occupied sites.

The entropy $s(\rho_x,\rho_y)$ is not concave everywhere. The true entropy $\bar{s}(\rho_x,\rho_y)$ is obtained by the Maxwell construction such that

$$\bar{s}(\rho_x,\rho_y) = \mathcal{CE}[s(\rho_x,\rho_y)], \tag{21}$$

where $\mathcal{CE}$ denotes the concave envelope.

The entropy may also be expressed in terms of the total density $\rho = \rho_x+\rho_y$ and the nematic order parameter ψ, defined as

$$\psi = \frac{\rho_x-\rho_y}{\rho}. \tag{22}$$

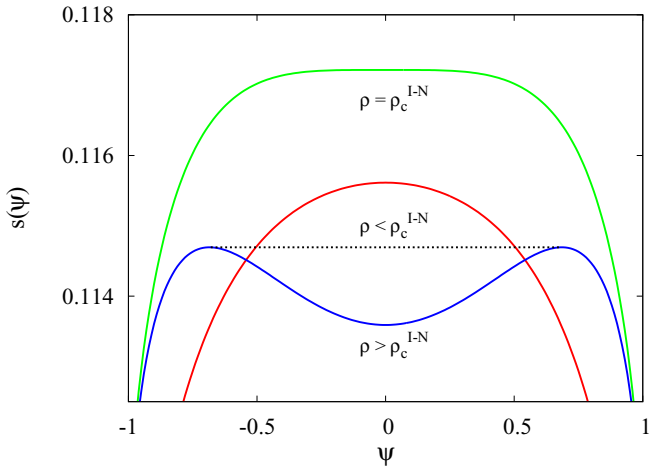

FIG. 7. (Color online) Entropy s as a function of the nematic order parameter ψ near the I-N transition ($\rho_c^{I-N} \approx 0.552$). The data are for $k = 4$ and $m = 2$. The dotted line denotes the concave envelope

ψ is zero in the isotropic phase and nonzero in the nematic phase. At a fixed density ρ, the preferred phase is obtained by maximizing $s(\psi)$ with respect to ψ. The transition density for the I-N transition is denoted by ρ_c^{I-N}. In Fig. 7 we show the plot of entropy $s(\psi)$ as a function of ψ, for three different densities near the I-N transition. For $\rho < \rho_c^{I-N}$ the entropy $s(\psi)$ is maximum at $\psi = 0$ i.e., $\rho_x = \rho_y$, corresponding to the isotropic phase. Beyond ρ_c^{I-N} the entropy develops two symmetric maxima at $\psi = \pm\psi_0$, where $\psi_0 = 0$ at $\rho = \rho_c^{I-N}$. $\psi_0 \neq 0$ i.e., $\rho_x \neq \rho_y$ corresponds to the nematic phase. The order parameter ψ grows continuously with density ρ. This is a typical signature of a continuous transition with two equivalent broken symmetry phases. The entropy $s(\rho,\psi)$ is invariant under the transformation $\psi \leftrightarrow -\psi$ and contains only even powers of ψ, when expanded about $\psi = 0$. The critical density ρ_c^{I-N} may be obtained by solving $d^2s/d\psi^2|_{\psi=0} = 0$ and is given by

$$\rho_c^{I-N} = \frac{2km}{mk^2 + m - k - 1}. \tag{23}$$

Asymptotic behavior of ρ_c^{I-N} is given by

$$\rho_c^{I-N} = \begin{cases} \frac{2}{k} + \frac{2}{mk^2} + O(k^{-3}), & k \to \infty,\ m \text{ fixed}, \\ \frac{2k}{1+k^2} + \frac{2k(1+k)}{(1+k^2)^2 m} + O(m^{-2}), & m \to \infty,\ k \text{ fixed}. \end{cases} \tag{24}$$

Thus, $A_1 = 2$.

When $m = 1$, the critical density $\rho_c^{I-N} = 2/(k-1)$, which matches with the exact calculation of ρ_c^{I-N} for the system of hard rods of length k on the RLTL [34]. It reflects that the Bethe approximations becomes exact on the RLTL. For $m = 1$, the nematic phase and hence the I-N transition exists for $k \geqslant k_{\min} = 4$. While for $m = 2$ and 3, $k_{\min} = 3$, for $m \geqslant 4$ the nematic phase exists even for $k = 2$.

B. Virial expansion

In this subsection we determine ρ_c^{I-N} using a standard virial expansion truncated at the second virial coefficient. We closely follow the calculations of Zwanzig for oriented hard rectangles in the continuum [38]. The excess free energy of the system of hard rectangles (relative to the ideal gas) may be expressed in terms of the virial coefficients and the density. We truncate the series at the second virial coefficient and study the I-N transition in the limit $k \to \infty$.

Consider a system of N rectangles on the square lattice of volume V. Each rectangle may be oriented along two possible directions. Setting $\beta = 1$, the configurational sum of the system is given by

$$Q_N = \frac{1}{N!2^N} \sum_{\mathbf{u}} \sum_{\mathbf{R}} \exp(-U_N), \tag{25}$$

where the sum over all possible positions and directions are denoted by $\sum_{\mathbf{R}}$ and $\sum_{\mathbf{u}}$, respectively, and U_N is the total interaction energy of all rectangles. The excess free energy (relative to the ideal gas) ϕ_N of the system of rectangles having fixed orientations is defined by

$$\exp[-\phi_N(\mathbf{u})] = \frac{1}{V^N} \sum_{\mathbf{R}} \exp(-\beta U_N). \tag{26}$$

As the rectangles having same orientation are indistinguishable, ϕ_N depends only on the fractions of the rectangles pointing along the two possible directions. If the number of rectangles oriented along direction i is denoted by N_i, we may rewrite the Eq. (25) using Eq. (26) as

$$\begin{aligned} Q_N &= \frac{V^N}{N!2^N} \sum_{N_1,N_2=0}^{N} \frac{N!}{N_1!N_2!} e^{-\phi_N(N_1,N_2)} \delta_{N_1+N_2,N} \\ &= \sum_{N_1=0}^{N} \sum_{N_2=0}^{N} W(N_1,N_2), \end{aligned} \tag{27}$$

where $\delta_{N_1+N_2,N}$ takes care of the constraint that the total number of rectangles is N and W is given by

$$W(N_1,N_2) = \frac{V^N}{2^N N_1!N_2!} \exp[-\phi_N(N_1,N_2)]. \tag{28}$$

In the thermodynamic limit $N \to \infty$ and $V \to \infty$, the above summation may be replaced by the largest summand $W_{\max}$ with negligible error. Thus the configurational free energy per particle is given by

$$F = -\lim_{N,V\to\infty} \frac{1}{N} \ln Q_N = -\lim_{N,V\to\infty} \frac{1}{N} W_{\max}. \tag{29}$$

The fractions of rectangles pointing in the i direction is denoted by $x_i = N_i/N$, such that $(x_1 + x_2) = 1$, and the number density of the rectangles is given by $N/V = \rho/m^2k$, where ρ is the total fraction of occupied sites. Equation (29) for the free energy may be expressed in terms of x_1 and x_2 as

$$\begin{aligned} F(x_1,x_2) = -1 + \ln 2 + \ln \frac{\rho}{m^2k} + \sum_{i=1}^{2} x_i \ln x_i \\ + \frac{1}{N}\phi_N(\rho,x_1,x_2). \end{aligned} \tag{30}$$

The virial expansion of the excess free energy ϕ_N, for a composition $\mathbf{x} = (x_1, x_2)$ of the rectangles is given by

$$-\frac{1}{N}\phi_N(\rho,\mathbf{x}) = \sum_{n=2} B_n(\mathbf{x}) \left(\frac{\rho}{m^2 k}\right)^{n-1}, \tag{31}$$

where

$$\begin{aligned} B_n(\mathbf{x}) &= \frac{1}{Vn!} \int \sum \prod f \\ &= \frac{1}{Vn!} \sum_{j=0}^{n} \binom{n}{j} x_1^{n-j} x_2^{j} B(n-j, j) \\ &= \frac{1}{V} \sum_{j=0}^{n} \frac{B(n-j,j)}{(n-j)!\,j!} x_1^{n-j} x_2^{j}, \end{aligned} \tag{32}$$

where $\int \sum \prod f$ is the standard abbreviation for the cluster integrals over the irreducible graphs consisting of n rectangles with composition $\mathbf{x}$ and f denotes the Mayer functions, defined as

$$f = \exp(-U) - 1, \tag{33}$$

where U is the interaction energy. Due to the hard-core exclusion, we have $U = \infty$ for any intersection or overlap among the rectangles, otherwise $U = 0$. Hence

$$f = \begin{cases} -1, & \text{for any intersection} \\ 0, & \text{otherwise} \end{cases} \tag{34}$$

$B(n-j, j)$ denotes the sum of the irreducible n-particle graphs for the composition where $(n-j)$ rectangles are oriented along the x direction and j rectangles are along the y direction.

As the total fraction $x_1 + x_2 = 1$, we set

$$\begin{aligned} x_1 &= x, \\ x_2 &= 1 - x. \end{aligned} \tag{35}$$

We consider up to the second virial coefficient and truncate the expansion in Eq. (31) at first order in ρ. From the definition of the virial coefficients in Eq. (32), we can easily infer that they are symmetric in the following way:

$$B(n_1, n_2) = B(n_2, n_1). \tag{36}$$

Using Eq. (32) and the above symmetry property of $B(n_1, n_2)$, we can rewrite Eq. (31) as

$$\begin{aligned} -\frac{1}{N}\phi_N \approx{}& \frac{1}{2V} B(2,0) \left(\frac{\rho}{m^2 k}\right) (2x^2 - 2x + 1) \\ &+ \frac{1}{V} B(1,1) \left(\frac{\rho}{m^2 k}\right) (x - x^2) + O(\rho^2). \end{aligned} \tag{37}$$

Now we evaluate the virial coefficients. From Eq. (34) we can see that f has nonzero contributions only when the rods intersect. Thus the calculation of the virial coefficients on a lattice turns out as the problem of counting the number of disallowed configurations. By definition

$$\begin{aligned} B(2,0) = B(0,2) &= \int d^2 R_1 \int d^2 R_2 \; f_{12}(2,0) \\ &= -V \times (2mk - 1) \times (2m - 1), \end{aligned} \tag{38}$$

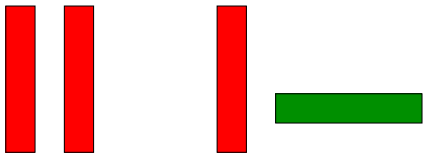

(a) (b)

FIG. 8. (Color online) Schematic diagram showing the orientations of two rectangles in the calculation of (a) $B(2,0)$ and (b) $B(1,1)$.

where $(2mk - 1) \times (2m - 1)$ is the number of disallowed configurations when both the rectangles are oriented along the same direction [see Fig. 8(a)]. Similarly,

$$\begin{aligned} B(1,1) &= \int d^2 R_1 \int d^2 R_2 \; f_{12}(1,1) \\ &= -V \times (m + mk - 1)^2, \end{aligned} \tag{39}$$

where $(m + mk - 1)^2$ is the number of disallowed configurations when the two rectangles are oriented along different directions [see Fig. 8(b)].

Substituting Eqs. (38) and (39) into Eq. (37), we find

$$\begin{aligned} -\frac{1}{N}\phi_N \approx{}& -\frac{1}{2}(2x^2 - 2x + 1)\left(\frac{\rho}{m^2 k}\right)(2m - 1)(2mk - 1) \\ &- (x - x^2)\left(\frac{\rho}{m^2 k}\right)(m + mk - 1)^2 + O(\rho^2). \end{aligned} \tag{40}$$

Now substituting Eq. (40) in Eq. (30), the expression for the free energy reduces to

$$\begin{aligned} F(x) = {}& -1 + \ln 2 + \ln \frac{\rho}{m^2 k} + x \ln x + (1 - x) \ln(1 - x) \\ &+ (x - x^2)\left(\frac{\rho}{m^2 k}\right)(m + mk - 1)^2 + \left(x^2 - x + \frac{1}{2}\right) \\ &\times \left(\frac{\rho}{m^2 k}\right)(2m - 1)(2mk - 1) + O(\rho^2). \end{aligned} \tag{41}$$

The preferred state at any fixed density is obtained by minimizing the free energy $F(x)$ with respect to x. For $\rho < \rho_c^{I-N}$, $F(x)$ is minimized for $x = 1/2$, corresponding to the isotropic phase, and beyond ρ_c^{I-N}, $F(x)$ is minimized for $x \neq 1/2$, corresponding to the nematic phase. Thus the system undergoes a transition from an isotropic phase to a nematic phase with increasing density. The I-N transition is found to be continuous with the critical density ρ_c^{I-N}.The expansion of the free energy $F(x)$ as a power series in x about $x = 1/2$ contains only even powers, and thus the critical density ρ_c^{I-N} may be determined by solving

$$\frac{d^2}{dx^2} F(x)|_{x=\frac{1}{2}} = 0. \tag{42}$$

By solving Eq. (42) for ρ, we find

$$\rho_c^{I-N} = \frac{2k}{(k-1)^2}, \tag{43}$$

which independent of m for all k. The asymptotic behavior of ρ_c^{I-N} is given by

$$\rho_c^{I-N} = \frac{2}{k} + \frac{4}{k^2} + O(k^{-2}), \quad \text{when } k \to \infty. \tag{44}$$

Comparing Eq. (24) and Eq. (44), we see that both the Bethe approximation and the virial theory predicts $\rho_c^{I-N} \approx A_1/k$ for $k \gg 1$, where $A_1 = 2$.

VI. SUMMARY AND DISCUSSION

For $k \geqslant 7$, the system of long, hard rectangles of size $m \times mk$ on the square lattice undergoes three entropy-driven phase transitions with density: first, from a low-density I phase to an intermediate-density N phase; second, from the N phase to a C phase; and, third, from the C phase to a high-density S phase [26]. In this paper we study the I-N and the N-C transition when $k \gg 1$. From extensive Monte Carlo simulations of systems with $m = 1$, 2, and 3, we establish that $\rho_c^{I-N} \approx A_1/k$, for $k \gg 1$, where A_1 is independent of m and is estimated to be 4.80 ± 0.05, the numerical value being consistent with that obtained from simulation of oriented lines [33]. The maximum value of k studied in the paper is 60, earlier simulations having been restricted up to $m = 1$ and $k = 12$ [40]. The I-N transition was also studied analytically using an *ad hoc* Bethe approximation and a truncated virial expansion. Both these theories support the numerical result $\rho_c^{I-N} \approx A_1/k$, for $k \gg 1$, where A_1 is independent of m. Within both these theories, we obtain $A_1 = 2$.

The Bethe approximation, while taking into account nearest-neighbor correlations, ignores other correlations and there appears to be no systematic way of improving the calculations to obtain better estimates of A_1. On the other hand, the virial expansion truncated at the second virial coefficient is known to become exact in three dimensions when $k \to \infty$. But in two dimensions, higher-order virial coefficients contributes significantly. To confirm this, we computed the higher-order virial coefficients. As $B_2 \sim k^2$ [see Eqs. (39)], in the limit $k \to \infty$, $B_2 \times \rho/k \sim O(1)$. We can rewrite Eq. (31) as

$$-\frac{1}{N}\phi_N(\mathbf{x}) \approx B_2(\mathbf{x})\frac{\rho}{m^2k} + \frac{B_3(\mathbf{x})}{[B_2(\mathbf{x})]^2}\left[B_2(\mathbf{x})\frac{\rho}{m^2k}\right]^2 + \frac{B_4(\mathbf{x})}{[B_2(\mathbf{x})]^3}\left[B_2(\mathbf{x})\frac{\rho}{m^2k}\right]^3 + O(\rho^4). \quad (45)$$

When $k \gg 1$, it can be verified that $B_3 \sim O(k^3)$ and hence $B_3/[B_2]^2 \sim O(1/k)$. Quite interestingly, we find $B_4 \sim O(k^6)$ and $B_4/[B_2]^3 \sim O(1)$. Thus B_4 will have non-negligible contribution to ρ_c^{I-N}. In general, $B_{2n} \sim O(k^{4n-2})$, implying all the even virial coefficients will have non-negligible contributions. Usually, the number of diagrams required to compute higher-order virial coefficients increase rapidly with order. However, here the number of diagrams are of order 1. Hence, it may be possible to determine A_1 exactly by taking into account all the even virial coefficients.

We also numerically investigated the asymptotic behavior of ρ_c^{N-C} for $m = 2$ and found $\rho_c^{N-C} \approx 0.73 + 0.23k^{-1}$ when $k \gg 1$, which is in qualitative agreement with the prediction of the Bethe approximation: $\rho_c^{N-C} \approx A_2 + A_3/k$, for $k \gg 1$, presented in Ref. [26]. For larger m, we expect the transition to become first order; however, the asymptotic result is likely to be qualitatively the same. Taking the limit $k \to \infty$, keeping m fixed, corresponds to a system of thin, long hard rectangles in the continuum. Thus, we expect the N-C transition to persist in continuum models.

Density-functional theory calculations for a system of hard rectangles with restricted orientation in the continuum, confined in a two-dimensional square nanocavity, predicts that the system will exhibit nematic, smectic, columnar, and solidlike phases, where the solidlike phase has both orientational and complete positional order [50]. In contrast, we do not find any evidence of smectic or solidlike phases when m or k tend to ∞, the continuum limit. In particular, on lattices the maximal density phase of a monodispersed system does not have orientational order [24,30]. Though we have considered only cases where the aspect ratio is an integer, most of the results will be also be true for the case when the aspect ratio is a rational number. In such a case, we expect that if the length and width are mutually prime, then the maximal density phase would be both spatially and orientationally disordered (not a sublattice phase). In the continuum, the aspect ratio could be irrational, too. In this case, it has been conjectured that there could be more transitions at densities close to 1 when the disordered phase will become unstable to a nematic or columnar phase [24]. For these reasons, it would be important to verify the phase diagram of hard rectangles with restricted orientation in a two-dimensional continuum through direct numerical simulations, similarly to the simulations for rectangles with continuous orientation [51–54].

We showed that the critical Binder cumulant for the N-C transition decreases as k^{-1} with increasing the aspect ratio k of the rectangles. The critical Binder cumulant in the Ising model on rectangular geometry decreases as α^{-1}, where α is the aspect ratio of the lattice [43]. Whether a mapping between k and α exists is an open question. Curiously, the critical Binder cumulant is zero when $k \to \infty$ (or $\alpha \to \infty$). In the Ising model, this has been interpreted as the absence of transition on one-dimensional geometries [43]. However, the hard-rectangle system shows a transition at $k \to \infty$. It is possible that in this limit, the fluctuations at the transition become Gaussian.

The critical density for the high-density C-S transition was argued to be of the form $1 - a/(mk^2)$ for $k \gg 1$, where a is a constant [26]. However, we could not numerically verify this claim as it becomes difficult to equilibrate the system at densities close to 1 due to the presence of long-lived metastable states. Thus, the Monte Carlo algorithm needs further improvement. One possible direction is the modification suggested in Ref. [29], where fully packed configurations are simulated using transfer matrices.

The hard-rectangle model may be generalized in different directions. Including attractive interaction results in phases with broken orientational and transitional symmetry even for dimers [55,56]. Such phases may also be seen in mixtures of hard particles, for example, dimers and squares [29]. Another generalization is to study polydispersed systems. In the continuum, polydispersity may result in reentrant nematic phase or two distinct nematic phases [57,58]. It would be interesting to see which features persist in the lattice version of rods [59,60] or rectangles. These are promising areas for further study.

ACKNOWLEDGMENTS

We thank W. Selke, D. Frenkel, D. Dhar, and J. F. Stilck for helpful discussions. We are grateful to an anonymous

referee for pointing out the omission of a factor of 2 in the virial expansion. The simulations were carried out on the supercomputing machine Annapurna at The Institute of Mathematical Sciences.

[1] D. E. Taylor, E. D. Williams, R. L. Park, N. C. Bartelt, and T. L. Einstein, Phys. Rev. B **32**, 4653 (1985).
[2] P. Bak, P. Kleban, W. N. Unertl, J. Ochab, G. Akinci, N. C. Bartelt, and T. L. Einstein, Phys. Rev. Lett. **54**, 1539 (1985).
[3] B. Dünweg, A. Milchev, and P. A. Rikvold, J. Chem. Phys. **94**, 3958 (1991).
[4] M. T. Koper, J. Electroanal. Chem. **450**, 189 (1998).
[5] A. Patrykiejew, S. Sokolowski, and K. Binder, Surf. Sci. Rep. **37**, 207 (2000).
[6] D.-J. Liu and J. W. Evans, Phys. Rev. B **62**, 2134 (2000).
[7] B. J. Alder and T. E. Wainwright, J. Chem. Phys. **27**, 1208 (1957).
[8] B. J. Alder and T. E. Wainwright, Phys. Rev. **127**, 359 (1962).
[9] D. Dhar, Phys. Rev. Lett. **49**, 959 (1982).
[10] D. Dhar, Phys. Rev. Lett. **51**, 853 (1983).
[11] D. C. Brydges and J. Z. Imbrie, J. Stat. Phys. **110**, 503 (2003).
[12] G. Parisi and N. Sourlas, Phys. Rev. Lett. **46**, 871 (1981).
[13] D. S. Gaunt and M. E. Fisher, J. Chem. Phys. **43**, 2840 (1965).
[14] A. Bellemans and R. K. Nigam, J. Chem. Phys. **46**, 2922 (1967).
[15] P. A. Pearce and K. A. Seaton, J. Stat. Phys. **53**, 1061 (1988).
[16] A. Baram and M. Fixman, J. Chem. Phys. **101**, 3172 (1994).
[17] X. Feng, H. W. J. Blöte, and B. Nienhuis, Phys. Rev. E **83**, 061153 (2011).
[18] K. Ramola and D. Dhar, Phys. Rev. E **86**, 031135 (2012).
[19] R. J. Baxter, J. Phys. A **13**, L61 (1980).
[20] O. J. Heilmann and E. Praestgaard, J. Stat. Phys. **9**, 23 (1973).
[21] R. Dickman, J. Chem. Phys. **136**, 174105 (2012).
[22] A. Verberkmoes and B. Nienhuis, Phys. Rev. Lett. **83**, 3986 (1999).
[23] B. C. Barnes, D. W. Siderius, and L. D. Gelb, Langmuir **25**, 6702 (2009).
[24] A. Ghosh and D. Dhar, Euro. Phys. Lett. **78**, 20003 (2007).
[25] J. Kundu, R. Rajesh, D. Dhar, and J. F. Stilck, Phys. Rev. E **87**, 032103 (2013).
[26] J. Kundu and R. Rajesh, Phys. Rev. E **89**, 052124 (2014).
[27] H. C. M. Fernandes, J. J. Arenzon, and Y. Levin, J. Chem. Phys. **126**, 114508 (2007).
[28] T. Nath and R. Rajesh, Phys. Rev. E **90**, 012120 (2014).
[29] K. Ramola, K. Damle, and D. Dhar, arXiv:1408.4943 (2014).
[30] P. G. de Gennes and J. Prost, *The Physics of Liquid Crystals* (Oxford University Press, Oxford, 1995), pp. 59–66.
[31] M. Disertori and A. Giuliani, Commun. Math. Phys. **323**, 143 (2013).
[32] D. A. Matoz-Fernandez, D. H. Linares, and A. J. Ramirez-Pastor, Euro. Phys. Lett **82**, 50007 (2008).
[33] T. Fischer and R. L. C. Vink, Euro. Phys. Lett. **85**, 56003 (2009).
[34] D. Dhar, R. Rajesh, and J. F. Stilck, Phys. Rev. E **84**, 011140 (2011).
[35] J. Kundu and R. Rajesh, Phys. Rev. E **88**, 012134 (2013).
[36] M. E. Zhitomirsky and H. Tsunetsugu, Phys. Rev. B **75**, 224416 (2007).
[37] L. Onsager, Ann. N.Y. Acad. Sci. **51**, 627 (1949).
[38] R. Zwanzig, J. Chem. Phys. **39**, 1714 (1963).
[39] G. J. Vroege and H. N. W. Lekkerkerker, Rep. Prog. Phys. **55**, 1241 (1992).
[40] D. A. Matoz-Fernandez, D. H. Linares, and A. J. Ramirez-Pastor, J. Chem. Phys. **128**, 214902 (2008).
[41] T. Nath, J. Kundu, and R. Rajesh, arXiv:1411.7831 (2014).
[42] J. Kundu, R. Rajesh, D. Dhar, and J. F. Stilck, AIP Conf. Proc. **1447**, 113 (2012).
[43] G. Kamieniarz and H. W. J. Blöte, J. Phys. A **26**, 201 (1993).
[44] W. Selke and L. N. Shchur, J. Phys. A **38**, L739 (2005).
[45] W. Selke, J. Stat. Mech. (2007) P04008.
[46] E. DiMarzio, J. Chem. Phys. **35**, 658 (1961).
[47] P. Centres and A. Ramirez-Pastor, Physica A **388**, 2001 (2009).
[48] D. H. Linares, F. Romá, and A. J. Ramirez-Pastor, J. Stat. Mech. (2008) P03013.
[49] E. P. Sokolova and N. P. Tumanyan, Liq. Cryst. **27**, 813 (2000).
[50] M. González-Pinto, Y. Martínez-Ratón, and E. Velasco, Phys. Rev. E **88**, 032506 (2013).
[51] M. A. Bates and D. Frenkel, J. Chem. Phys **109**, 6193 (1998).
[52] M. A. Bates and D. Frenkel, J. Chem. Phys **112**, 10034 (2000).
[53] K. W. Wojciechowski and D. Frenkel, Comput. Methods Sci. Tech. **10**, 235 (2004).
[54] A. Donev, J. Burton, F. H. Stillinger, and S. Torquato, Phys. Rev. B **73**, 054109 (2006).
[55] F. Alet, J. L. Jacobsen, G. Misguich, V. Pasquier, F. Mila, and M. Troyer, Phys. Rev. Lett. **94**, 235702 (2005).
[56] S. Papanikolaou, D. Charrier, and E. Fradkin, Phys. Rev. B **89**, 035128 (2014).
[57] N. Clarke, J. A. Cuesta, R. Sear, P. Sollich, and A. Speranza, J. Chem. Phys **113**, 5817 (2000).
[58] Y. Martínez-Ratón and J. A. Cuesta, J. Chem. Phys **118**, 10164 (2003).
[59] D. Ioffe, Y. Velenik, and M. Zahradnik, J. Stat. Phys. **122**, 761 (2006).
[60] J. F. Stilck and R. Rajesh, Phys. Rev. E **91**, 012106 (2015).